ARTICLES

Femtosecond Time-Resolved Fluorescence Study of Photoisomerization of *trans*-Azobenzene

Tatsuya Fujino,[†] Sergei Yu. Arzhantsev,[†] and Tahei Tahara*[,†,‡]

Institute for Molecular Science (IMS), Myodaiji, Okazaki 444-8585, Japan, and Molecular Spectroscopy Laboratory, The Institute of Physical and Chemical Research (RIKEN), Hirosawa, Wako 351-0198, Japan

Received: March 22, 2001; In Final Form: June 11, 2001

The electronic relaxation and isomerization mechanism of *trans*-azobenzene after the $S_2(\pi\pi^*) \leftarrow S_0$ photoexcitation were investigated in solution by steady-state and femtosecond time-resolved fluorescence spectroscopy. In the steady-state fluorescence spectrum, two bands were observed with their peaks at ∼390 nm (∼25 750 cm^{-1}) and ∼665 nm (∼15 000 cm^{-1}). These fluorescence bands showed good mirror images of the $S_2(\pi\pi^*) \leftarrow S_0$ and $S_1(n\pi^*) \leftarrow S_0$ absorption bands, so that they were assigned to the fluorescence from the $S_2(\pi\pi^*)$ and $S_1(n\pi^*)$ states having "planar" structures. The lifetimes of the S_2 and S_1 states were determined as ∼110 fs (S_2) and ∼500 fs (S_1) by time-resolved measurements. The quantum yield of the $S_2 \rightarrow S_1$ electronic relaxation was evaluated by comparing the intensity of the S_2 and S_1 fluorescence, and it was found to be almost unity. This implies that almost all molecules photoexcited to the $S_2(\pi\pi^*)$ state are relaxed to the "planar" $S_1(n\pi^*)$ state. The present fluorescence data clarified that the isomerization following $S_2(\pi\pi^*)$ photoexcitation takes place after the $S_2 \rightarrow$ planar S_1 electronic relaxation and that the rotational isomerization pathway starting directly from the $S_2(\pi\pi^*)$ state does not exist. It was thus indicated that the isomerization mechanism of azobenzene is the inversion isomerization occurring in the S_1 state, regardless of difference in initial photoexcitation. The relaxation pathways in the S_1 state were also discussed on the basis of spectroscopic and photochemical data.

1. Introduction

Azobenzene and its derivatives are typical molecules showing cis−trans photoisomerization, and they have been attracting much interest not only from the viewpoint of fundamental photochemistry but also for their high potential in industrial applications. For example, azobenzene derivatives are considered to be useful as materials for the liquid crystal, light-driven switches[1,2] and image storage devices[3] having fast response time. Functions in these industrial applications are based on cis−trans photoisomerization of the azobenzene moiety so that the elucidation of the isomerization mechanism of azobenzene is very important. Photoisomerization as well as other properties of *trans*-azobenzene has been extensively investigated by variety of physicochemical methods such as UV−visible absorption,[4−7] Raman,[8,9] NMR,[10] and theoretical calculations.[11,12] So far, it has been said that photoisomerization of *trans*-azobenzene (we simply call it azobenzene hereafter) takes place with two different isomerization mechanisms (Scheme 1); with $S_1(n\pi^*) \leftarrow S_0$ excitation the isomerization occurs by inversion around one N atom (inversion mechanism), whereas rotation around the NN double bond is induced by $S_2(\pi\pi^*) \leftarrow S_0$ excitation (rotation mechanism). The inversion mechanism was proposed and experimentally demonstrated by Rau and Lüddecke.[4] They synthesized azobenzene derivatives in which the rotational motion was prohibited, but they observed the same photoisomerization quantum yield as for azobenzene itself. On the other hand, the rotational mechanism after S_2 photoexcitation has not been well-proved, although it is the established mechanism for isomerization around the C=C double bond which is induced by $\pi\pi^*$ excitation.[13−16]

SCHEME 1

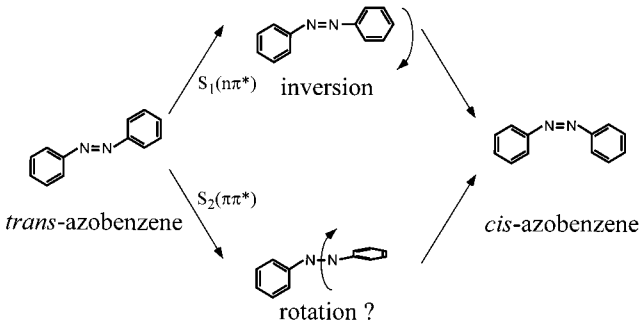

The photoisomerization mechanism and dynamics can be more directly examined by time-resolved spectroscopy. However, the number of reports is still limited for azobenzene because the isomerization process takes place very rapidly. Recently, femtosecond UV−visible absorption measurements[17−19] were carried out with the $S_2(\pi\pi^*) \leftarrow S_0$ excitation and the following dynamics was observed. Immediately after photoexcitation, a transient absorption assignable to the $S_2(\pi\pi^*)$ state appears around ∼475 nm. After the decay of this transient (<200 fs), another transient absorption peaked around 400 nm appears and it decays with a time constant of ∼1 ps in hexane. Besides,

* To whom correspondence should be addressed.
† IMS.
‡ RIKEN.

10.1021/jp0110713 CCC: $20.00
Published on Web 08/14/2001

a minor slow decay component having a lifetime of ~16 ps is also observed at ~400 nm. Lednev et al. interpreted the observed dynamics according to the rotational mechanism. They assigned the 400-nm transient(s) to the twisted excited states in the S_2 (lifetime ~1 ps) and S_1 (~16 ps) states that are supposed to appear in the rotational isomerization pathway. The time-resolved absorption study successfully revealed the time scale of the photoisomerization process of azobenzene. However, the interpretations of the experimental data were questionable because absorption spectra cannot provide clear information about the molecular structure.

Unambiguous assignments of the dynamics observed after S_2 photoexcitation, especially the assignment of the 400-nm transient, were made by picosecond time-resolved Raman spectroscopy,[20] which affords direct information about the molecular structure[21−23] as well as the vibrational relaxation process. The results of the Raman study can be summarized as follows. First, it was found that the lifetime of the 400-nm transient strongly depends on the solvent and that the lifetime becomes as long as 13 ps in ethylene glycol. This means that the 400-nm transient is not the S_2 state but the S_1 state. Second, the NN stretching frequency of the 400-nm transient (the S_1 state) was determined by the ^{15}N-substitution, and it was clarified that the frequency in the S_1 state is very close to that of the S_0 state (1428 cm^{-1} in S_1 and 1440 cm^{-1} in S_0). This implies that the NN bond retains a double bond character in the S_1 state so that the S_1 state is not the twisted state but has a "planar" structure around the central NN bonding. Third, in the time-resolved anti-Stokes Raman measurements, it was observed that the hot bands due to the S_0 state appear in accordance with the decay of the S_1 state and that the S_0 hot bands disappear with a time constant of ~16 ps. Therefore the 16-ps dynamics, which was also observed in transient absorption measurements, can be straightforwardly assigned to the vibrational cooling process in the S_0 state. (This assignment was consistent with the result of the femtosecond time-resolved infrared study.[24]) The picosecond Raman study clarified that the dynamics observed in the femtosecond and picosecond time region is the $S_2 \rightarrow S_1 \rightarrow S_0$ electronic relaxation process that takes place in a molecule preserving essentially planar structure around NN bonding.

The planar S_1 state appearing after S_2 photoexcitation is highly likely the same state as that prepared by the direct $S_1(n\pi^*) \leftarrow S_0$ photoexcitation. Therefore, from the viewpoint of photoisomerization, the results of the picosecond Raman study suggested that the inversion isomerization in the S_1 state also takes part in the isomerization following the S_2 excitation. So far, it has been believed that, in the case of S_2 photoexcitation, the excitation induces the rotation around the NN double bond to generate the twisted excited state and then the cis isomer is produced exclusively from this twisted intermediate (the rotational pathway). Therefore, we now need to discuss which is the major isomerization pathway after $S_2(\pi\pi^*)$ photoexcitation, the rotational isomerization directly starting from the $S_2(\pi\pi^*)$ state or the inversion isomerization that takes place after electronic relaxation to the planar S_1 state. In other words, we need to reconsider the existence of the S_2 rotational pathway itself.

In this paper, we report the femtosecond time-resolved, as well as steady-state, fluorescence study of trans-azobenzene with $S_2(\pi\pi^*)$ photoexcitation. We measured the spectrum and lifetime of the S_2 and S_1 fluorescence and confirmed the arguments that were made in the previous picosecond Raman study. More importantly, we evaluated the quantum yield of the $S_2 \rightarrow S_1$ vertical relaxation process by comparing the relative intensity between the S_2 and S_1 fluorescence with that between the S_2 and S_1 absorption. The obtained fluorescence data clearly show that the S_2 state is almost exclusively relaxed to the planar S_1 state and that the rotational isomerization pathway starting directly from the S_2 state *does not* exist.

2. Experimental Section

The experimental setup used for femtosecond time-resolved fluorescence measurements has been already described elsewhere.[25,26] Briefly, a mode-locked Ti:sapphire laser (Spectra-Physics, Tsunami) that was pumped by an Ar^+ laser (Spectra-Physics, Beamlok 2060−10SA) provided femtosecond pulses (840 nm, 10 nJ, 60 fs) at a repetition rate of 82 MHz. The output from the Ti:sapphire oscillator laser was frequency doubled by a 0.5-mm LBO crystal (420 nm, 1.8 nJ) and then tripled by a 1-mm BBO crystal (280 nm, 560 pJ). The generated third harmonic pulses were focused onto a thin-film-like jet stream of a sample solution for photoexcitation. The residual fundamental pulses after the third harmonics generation were used as gate pulses for the fluorescence up-conversion process. The fluorescence from the sample was collected by using an elliptic mirror and then focused into a 0.5-mm BBO crystal to be mixed with the gate pulse. The up-converted signal was separated by filters and a monochromator (Jovin-Yvon, HR-320) and it was detected by a photomultiplier (Hamamatsu, H585) with a photon counter (Stanford Research Systems, SR400). The fluorescence was measured with the magic angle condition by tilting the excitation polarization with respect to the gate polarization. The time resolution of the time-resolved fluorescence measurement was evaluated by the cross-correlation trace between the excitation and gate pulses, and it was typically ~230 fs (fwhm). All measurements were performed at room temperature.

Steady-state fluorescence spectrum was measured using the detection system of our picosecond time-resolved Raman apparatus.[16] The third harmonic pulses of the output from a picosecond mode-locked Ti:sapphire laser (280 nm, 11 pJ, 1.8 ps at a repetition rate of 90 MHz) were focused onto a thin-film-like jet stream of a sample solution with a quartz lens (f = 50 mm) for photoexcitation. The fluorescence signals were analyzed with a polychromator (Jovin-Yvon, HR-320) and detected by a liquid nitrogen cooled CCD (Princeton Instruments, LN/CCD-1100PB). The steady-state measurement was also carried out with the magic angle condition. Sensitivity correction of the detection system was carried out using a standard lamp (Ushio, 3230 K color temperature), and the spectral distortion due to the self-absorption effect was also corrected. The wavelength resolution of the steady-state measurements was ~1 nm. Steady-state absorption spectra were measured with a commercial spectrometer (Hitachi, U-3400).

Azobenzene (*trans*) was purchased from Wako Pure Chemical Industries and was recrystallized 3 times from methanol. The purified sample was sufficiently dried in a drybox before use. The samples were dissolved in hexane (Wako Pure Chemical Industries, HPLC grade) and the solutions with a concentration of 5.0 x 10^{-3} mol dm^{-3} were used for the time-resolved and steady-state fluorescence measurements. A fresh sample solution was prepared for each measurement.

3. Results and Discussions

3.1. Steady-State Fluorescence Spectrum. Ground-state azobenzene shows two absorption bands in the UV−visible region. The intense absorption band peaked at ~315 nm (~31 750 cm^{-1}) is assigned to the $S_2(\pi\pi^*) \leftarrow S_0$ transition and

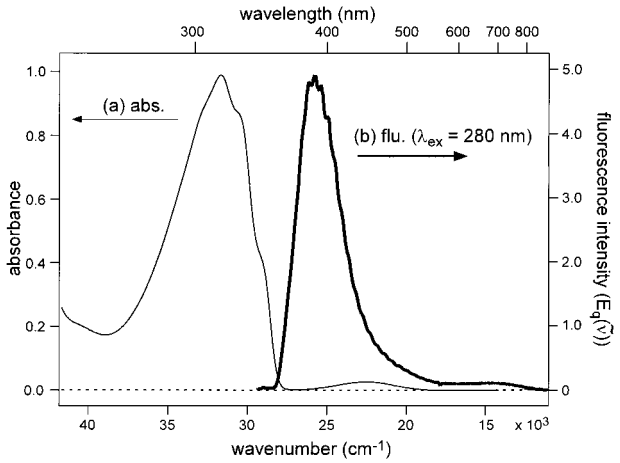

Figure 1. UV−visible absorption (left, a) and the steady-state fluorescence spectrum obtained with the excitation at 280 nm (right, b) in hexane (5.0 x 10^{-3} mol dm^{-3}). For the fluorescence spectrum, the spectral distortion due to the self-absorption effect as well as the detector sensitivity has been corrected.

the weak band peaked at ∼450 nm (∼22 220 cm^{-1}) to the S_1-(nπ^*) ← S_0 transition. We measured steady-state fluorescence spectra with 280-nm photoexcitation. This excitation wavelength corresponds to the blue side of the $S_2(\pi\pi^*) \leftarrow S_0$ absorption ($\epsilon_{280} \approx 10\,000$ mol^{-1} dm^3 cm^{-1}), and the molecules are initially photoexcited to the $S_2(\pi\pi^*)$ state. The steady-state fluorescence spectrum measured from a hexane solution (5.0 x 10^{-3} mol dm^{-3}) is compared with the absorption spectrum in Figure 1. The fluorescence spectrum is represented as the photon-number intensity in the frequency space in this figure. As clearly seen, the intensity maximum of the steady-state fluorescence is located at ∼390 nm (∼25 750 cm^{-1}), which is energetically higher than the $S_1(n\pi^*) \leftarrow S_0$ transition. In addition, the main fluorescence band shows a good mirror image of the $S_2(\pi\pi^*) \leftarrow S_0$ absorption band. These facts indicate that the major component of the steady-state fluorescence is not the S_1 fluorescence but the S_2 fluorescence. However, the fluorescence spectrum extends to the red region and it exhibits a very weak peak around ∼665 nm (∼15 000 cm^{-1}). This second fluorescence band shows a mirror image of the $S_1(n\pi^*) \leftarrow S_0$ absorption band so that it is attributable to the S_1 fluorescence. (This assignment is further confirmed by the time-resolved measurements described in the next section.) The observed spectral feature directly shows that the steady-state fluorescence spectrum consists of two components, the $S_2(\pi\pi^*)$ and the $S_1(n\pi^*)$ fluorescence. The appearance of the S_1 fluorescence after S_2 photoexcitation means that the planar S_1 state (the Franck−Condon active state from the S_0 state) is certainly produced by the $S_2 \rightarrow S_1$ electronic relaxation, as argued by the previous picosecond time-resolved Raman study.[20] Although azobenzene is one of the most fundamental molecules, to the authors' best knowledge, no reliable steady-state fluorescence spectrum had been reported because of its very low quantum yield.[27,28] In the present measurement, we could successfully observe fluorescence from azobenzene, taking advantage of a highly sensitive multichannel detection system. The steady-state fluorescence spectrum obtained in the present measurements is significantly different from the time-resolved spectrum taken with the Kerr-gate method.[29,30]

It is noted that the steady-state fluorescence of *trans*-azobenzene does not obey Kasha's rule because the S_2 fluorescence appears with much higher intensity than the S_1 fluorescence. As clearly demonstrated by our recent femtosecond fluorescence study,[31] fluorescence from highly excited singlet (S_n) states are observable in the femtosecond time region, even

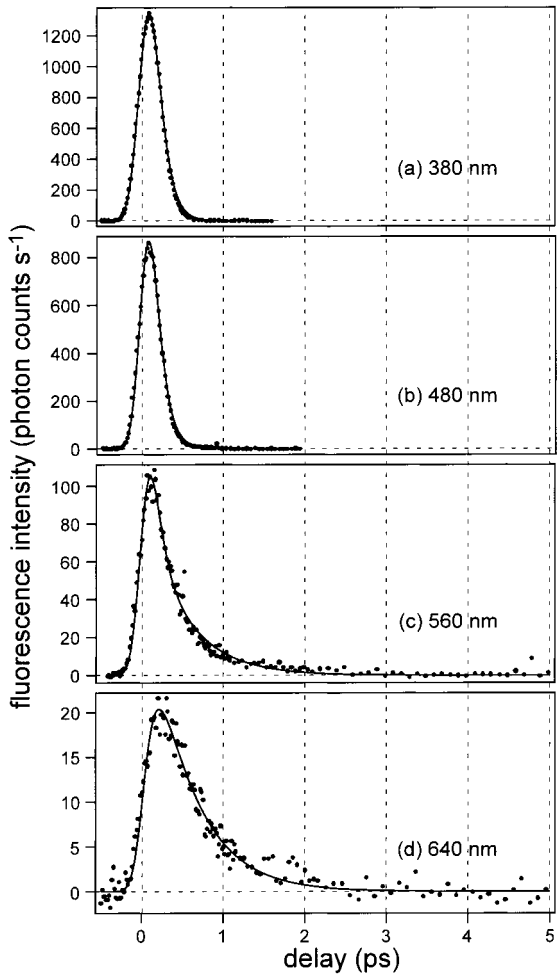

Figure 2. Femtosecond time-resolved fluorescence signals obtained from azobenzene in hexane (5.0 x 10^{-3} mol dm^{-3}, 280-nm excitation) at 380 nm (a), 480 nm (b), 560 nm (c), and 640 nm (d). The dotted circles are the experimental data, and the solid curves are the results of the fitting analysis. The time resolution of the measurements is ∼230 fs.

if they are not well recognized in steady-state fluorescence spectra. In usual cases, the lifetime of the S_n state is so short that the S_n fluorescence becomes negligibly weak compared with long-lived S_1 fluorescence in the (time-integrated) steady-state fluorescence spectrum. In the case of azobenzene, however, the S_1 fluorescence is extremely weak even in the time-integrated spectrum because of its very short lifetime and its optically forbidden nature. As a consequence, the S_2 fluorescence becomes the major component although the quantum yield of the S_2 fluorescence is very low as in usual molecules that obey Kasha's rule.

3.2. Time-Resolved Fluorescence. Femtosecond time-resolved fluorescence after $S_2(\pi\pi^*)$ photoexcitation was measured from a hexane solution (5.0 x 10^{-3} mol dm^{-3}) for a wide wavelength range from 340 to 680 nm by fluorescence up-conversion. The temporal behavior of the fluorescence signals varies with the change of wavelength, reflecting the dual nature of the fluorescence of azobenzene. Four typical time-resolved fluorescence traces are shown in Figure 2. The fluorescence decay at 380 nm, which is around the peak of S_2 fluorescence, looks close to the cross-correlation trace. It indicates that the lifetime of the S_2 state is comparable with the instrumental response. Fluorescence in the near-ultraviolet region (340−420 nm), which we assign to the S_2 fluorescence, exhibits almost the same temporal behavior. The second slower fluorescence

component becomes noticeable in the longer wavelength region. In the decay at 560 nm, the amplitude of the second component becomes comparable to that of the ultrafast S_2 fluorescence component, and then it becomes predominant at 640 nm, which corresponds to the peak of the weak fluorescence band assigned to the S_1 fluorescence. We checked the concentration dependence of the fluorescence signals for 5 x 10^{-3}, 1 x 10^{-3}, and 5 x 10^{-4} mol dm^{-3} samples and observed indistinguishable fluorescence dynamics. This assured us that there is no effect due to aggregation under the present experimental condition. (The absence of the azobenzene aggregates was also confirmed by checking steady-state UV−visible absorption spectra.) The obtained time-resolved fluorescence data clearly showed that the fluorescence consists of the S_2 and S_1 fluorescence and confirmed our assignment for the fluorescence bands in the steady-state spectrum. The time-resolved fluorescence signals decayed to the dark level within 5 ps, indicating that there is no other long-lived fluorescent state.

To obtain quantitative information from the fluorescence data, we carried out a global fitting analysis of the time-resolved fluorescence traces on the basis of the following relaxation scheme,

$$\begin{array}{ccccc} S_2 & \xrightarrow{k_{vert}} & S_1 & \xrightarrow{k_{S1}} & \\ & \searrow^{k_{ROT}} & & & \end{array} \qquad (1)$$

The observed time-resolved fluorescence intensity is the sum of the S_2 fluorescence and S_1 fluorescence so that it can be described as follows,

$$R(\tilde{\nu},t) = R_{S_2}(\tilde{\nu},t) + R_{S_1}(\tilde{\nu},t) = a_{S_2}(\tilde{\nu})\exp(-k_{S_2}t) + a_{S_1}(\tilde{\nu})\Phi k_{S_2}/(k_{S_2} - k_{S_1})\{\exp(-k_{S_1}t) - \exp(-k_{S_2}t)\} \quad (2)$$

where

$$k_{S_2} = k_{vert} + k_{ROT}, \quad \Phi = k_{vert}/(k_{vert} + k_{ROT})$$

Here, $a_{S_2}(\tilde{\nu})$, $a_{S_1}(\tilde{\nu})$ denote the intrinsic fluorescence intensity (transition probabilities) at wavenumber $\tilde{\nu}$ of the two fluorescence states, and k_{S_2}, k_{S_1} represent their population relaxation rates. The population relaxation rate of the S_2 state (k_{S2}) is the sum of the $S_2 \rightarrow S_1$ electronic relaxation rate (k_{vert}) and the rate of the other relaxation pathways (k_{ROT}), including the rotational isomerization in the S_2 state as well as the direct nonradiative $S_2 \rightarrow S_0$ relaxation. Thus, the Φ value represents the quantum yield of the $S_2 \rightarrow S_1$ electronic relaxation that generates the planar S_1 state. The fitting analysis for the observed fluorescence traces was made using a convoluted form of $R(\tilde{\nu},t)$ with a normalized instrumental response function (a Gaussian having fwhm of 228 fs). The results of the fitting are shown with solid curves in Figure 2. The observed data were well reproduced by the calculated curves, and we obtained the lifetimes of the S_2 and S_1 fluorescence as ~110 fs ($1/k_{S_2}$) and ~500 fs ($1/k_{S_1}$), respectively. We also determined the amplitude of each component, $a_{S_2}(\tilde{\nu})$ and $a_{S_1}(\tilde{\nu})\Phi$, as functions of wavenumber. When we normalize the time-resolved fluorescence intensity measured at different wavelengths (or frequencies), the $a_{S_2}(\tilde{\nu})$ and $a_{S_1}(\tilde{\nu})\Phi$ values represent the S_2 and S_1 fluorescence spectra. We normalized time-resolved fluorescence signals using the steady-state fluorescence spectrum.[25,26,31−33] By using the parameters determined by the fitting analysis, we could successfully decompose the steady-state fluorescence spectrum into the S_2 and S_1 fluorescence components, as shown in Figure 3.

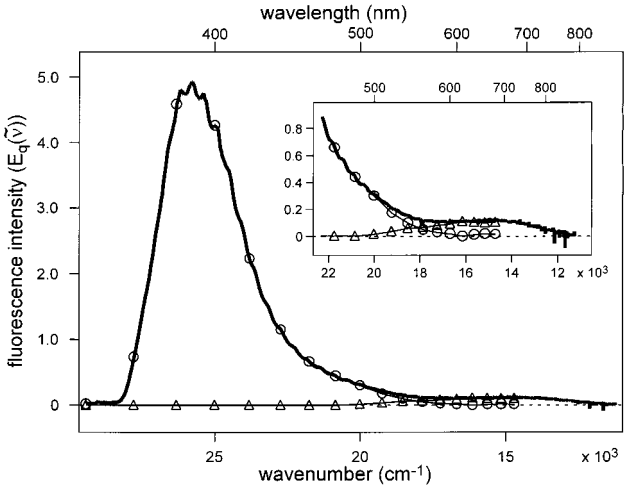

Figure 3. Time-integrated spectra of the $S_2(\pi\pi^*)$ and $S_1(n\pi^*)$ fluorescence reconstructed from the time-resolved fluorescence signals. The same figure is expanded in the inset. The steady-state fluorescence spectrum is shown with a solid curve for comparison. Open circles and open triangles represent the decomposition into the S_2 and S_1 fluorescence, respectively.

3.3. The $S_2 \rightarrow S_1$ Relaxation Quantum Yield. The $S_2 \rightarrow S_1$ relaxation quantum yield, Φ, is the key when we discuss the isomerization mechanism after S_2 excitation, because the rotational isomerization starts from the S_2 state whereas the inversion takes place in the S_1 state after electronic relaxation. Since the S_1 fluorescence intensity depends on how many molecules are relaxed to the S_1 state, the fluorescence spectrum (or, more specifically, the intensity ratio between the S_2 and S_1 fluorescence) is very sensitive to the Φ value. Thus we can evaluate the $S_2 \rightarrow S_1$ relaxation quantum yield from the obtained fluorescence data.

By integrating the two terms in formula 2 in the time and frequency spaces, we obtain the following expression for the integrated intensity of the S_2 and S_1 fluorescence,

$$I_{S_2} = \int_0^{+\infty} d\tilde{\nu} \int_0^{+\infty} dt\, R_{S_2}(\tilde{\nu},t) = \frac{1}{k_{S_2}} \int_0^{+\infty} a_{S_2}(\tilde{\nu})\, d\tilde{\nu} \quad (3A)$$

$$I_{S_1} = \int_0^{+\infty} d\tilde{\nu} \int_0^{+\infty} dt\, R_{S_1}(\tilde{\nu},t) = \Phi \frac{k_{S_2}}{k_{S_2} - k_{S_1}} \left(\frac{1}{k_{S_1}} - \frac{1}{k_{S_2}}\right) \int_0^{+\infty} a_{S_1}(\tilde{\nu})\, d\tilde{\nu} \quad (3B)$$

As described in the previous section, the $a_{S_2}(\tilde{\nu})$ and $a_{S_1}(\tilde{\nu})$ values represent the intrinsic fluorescence transition probability of the S_2 and S_1 state at frequency $\tilde{\nu}$. Thus, the integration of the a_{S_i} (i = 1, 2) value in the frequency space yields a quantity proportional to the radiative decay rate, and hence it can be related to the oscillator strength,

$$\int_0^{+\infty} a_{S_i}(\tilde{\nu})\, d\tilde{\nu} \propto \tilde{\nu}_{S_i}^{\,2} f_{S_i} \qquad (4)$$

Here, $\tilde{\nu}_{S_i}$ is the peak frequency of the $S_i \rightarrow S_0$ fluorescence and f_{S_i} is the oscillator strength of the transition between the S_i and S_0 states. Combining formulas 3A, 3B, and 4, we obtain the following expression for the $S_2 \rightarrow S_1$ electronic relaxation quantum yield Φ,

$$\Phi = \left(\frac{I_{S_1}}{I_{S_2}}\right)\left(\frac{k_{S_1}}{k_{S_2}}\right)\left(\frac{\int_0^{+\infty} a_{S_2}(\tilde{\nu})\, d\tilde{\nu}}{\int_0^{+\infty} a_{S_1}(\tilde{\nu})\, d\tilde{\nu}}\right) = \left(\frac{I_{S_1}}{I_{S_2}}\right)\left(\frac{k_{S_1}}{k_{S_2}}\right)\left(\frac{\tilde{\nu}_{S_2}^{\,2}}{\tilde{\nu}_{S_1}^{\,2}}\right)\left(\frac{f_{S_2}}{f_{S_1}}\right) \quad (5)$$

TABLE 1: Assignments and Properties of the Two Fluorescence Decay Components

	component	
	$S_2(\pi\pi^*)$	$S_1(n\pi^*)$
peak wavelength, nm	390	665
Lifetime, ps	~0.110	~0.500
oscillator strength	0.51	0.01
radiative lifetime,[a] ns	4.4	670
fluorescence quantum yield[b]	2.53×10^{-5}	7.54×10^{-7}

[a] Radiative lifetime, τ_{ri}, is related to the oscillator strength value, f_i, as $\tau_{ri} = 1.499\ \text{cm}^{-2}\ \text{s}/\tilde{\nu}^2 f_i$. [b] Fluorescence quantum yield is the ratio of fluorescence lifetime to the radiative lifetime.

All the values on the right side of this formula can be obtained from the experimental data, so that we can evaluate the Φ value. The integrated intensities of the S_2 and S_1 fluorescence, I_{S_2} and I_{S_1}, were obtained from the decomposed spectra of the steady-state fluorescence shown in Figure 3, and the ratio of (I_{S_1}/I_{S_2}) was determined to be 0.032. The oscillator strength values of the $S_2(\pi\pi^*) \leftarrow S_0$ and the $S_1(n\pi^*) \leftarrow S_0$ transitions can be determined from the absorption spectrum by using the following formula,[34]

$$f = (4.32 \times 10^{-9}) \int \epsilon(\tilde{\nu})\, d\tilde{\nu} \qquad (6)$$

where $\epsilon(\tilde{\nu})$ is the molar absorption coefficient at frequency $\tilde{\nu}$. The oscillator strength of the $S_1(n\pi^*) \leftarrow S_0$ transition was evaluated as 0.010 from the absorption spectra shown in Figure 1.[35] For the S_2 $(\pi\pi^*) \leftarrow S_0$ transition, we integrated absorption coefficient over the region from 257 to 370 nm and obtained an oscillator strength value of 0.511. Then, the oscillator strength ratio between the $\pi\pi^*$ and $n\pi^*$ transitions, f_{S_2}/f_{S_1}, was determined to be 51.1. The other parameters used for the evaluation of the Φ value were already given, and they are as follows: $1/k_{S_2} = 0.112$ ps, $1/k_{S_1} = 0.502$ ps, $\tilde{\nu}_{S_2} = 25750\ \text{cm}^{-1}$, and $\tilde{\nu}_{S_1} = 15000\ \text{cm}^{-1}$. Consequently, we obtained a value of 1.07 (± 0.15) for the $S_2 \rightarrow S_1$ electronic relaxation quantum yield, Φ. The obtained Φ value can be regarded as unity within error, which means that the photoexcited S_2 state is almost exclusively relaxed to the planar S_1 state. Therefore, it is concluded that the rotational isomerization pathway that directly starts from the S_2 state does not exist, or, even if it exists, it is a very minor pathway.

Several important properties of the S_2 and S_1 states were also evaluated during the evaluation of the Φ value. They are listed in Table 1.

3.4. Relaxation and Isomerization Pathway of *trans*-Azobenzene after S_2 Excitation. The present fluorescence study clarified the relaxation process of azobenzene after the $S_2(\pi\pi^*) \leftarrow S_0$ excitation and afforded very important information to consider the isomerization mechanism of this fundamental molecule. The essential points of the results are summarized as follows. The steady-state fluorescence spectrum exhibits both S_2 fluorescence ($\lambda_{max} \sim 390$ nm) and S_1 fluorescence ($\lambda_{max} \sim 665$ nm), and these two fluorescence bands show good mirror images of the $S_2(\pi\pi^*) \leftarrow S_0$ and $S_1(n\pi^*) \leftarrow S_0$ absorption bands. Therefore, the fluorescing states are assigned to the S_2 and S_1 states that have planar structures around the central N=N bond. The lifetimes of the S_2 and S_1 states are determined to be ~110 fs (S_2) and ~500 fs (S_1) by fluorescence up-conversion measurements. The quantum yield of the $S_2 \rightarrow$ planar S_1 relaxation process is found to be almost unity, which indicates that the molecules in the S_2 state are almost exclusively relaxed to the planar S_1 state. These fluorescence data disclose that the rotational isomerization pathway starting directly from the S_2 state is negligible and that the isomerization following S_2 photoexciation actually takes place in the S_1 state after the electronic relaxation. It has been experimentally demonstrated that the isomerization in the S_1 state occurs by the inversion mechanism.[4] Thus, it can be concluded that the isomerization of azobenzene occurs by inversion regardless of the difference in initial photoexcitation. Therefore, the present results strongly indicate that the isomerization mechanism after the S_2 photoexcitation is the same as the mechanism following direct $S_1 \leftarrow S_0$ photoexcitation. In our previous work using picosecond time-resolved Raman spectroscopy,[20] we argued that the isomerization in the S_1 state also contributes to the isomerization following S_2 photoexcitation. Now, we can conclude that this isomerization pathway, the isomerization after $S_2 \rightarrow S_1$ electronic relaxation, is in fact the major isomerization pathway after the S_2 photoexcitation. The planar S_1 state observed by time-resolved absorption, Raman and fluorescence spectroscopy is assigned to the transient species from which the inversion isomerization starts. The relaxation and isomerization pathways following S_2 photoexcitation of azobenzene are sketched in Figure 4.

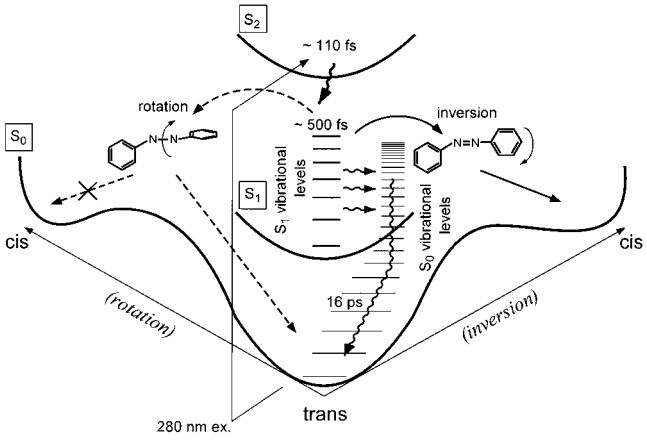

Figure 4. Schematic diagram of the relaxation and isomerization pathway of *trans*-azobenzene after the $S_2(\pi\pi^*) \leftarrow S_0$ photoexcitation in hexane. See text.

The isomerization mechanism of azobenzene was originally discussed on the basis of the isomerization quantum yield. This photochemical quantity was measured in several solvents, and it was reported to be 0.1−0.15 for S_2 photoexcitaion and 0.24−0.31 for S_1 photoexcitation.[36−38] Obviously, the isomerization quantum yield significantly depends on the excitation energy and the S_2 excitation gives almost the half-value of the S_1 excitation. This difference in the quantum yield was the major reason of the argument that the isomerization mechamism after S_2 photoexcitation is different from the mechanism following S_1 photoexcitation.[4] More specifically, it was said that the S_2 photoexcitation induces rotation around the NN double bond to generate the twisted excited state and the S_0 cis isomer is produced from this twisted intermediate with a quantum yield of ~0.1 (rotational isomerization). Since our study has clearly excluded the existence of this rotational pathway, we now need to reconsider and rationalize the difference in the isomerization quantum yield in a way consistent with the spectroscopic data, especially with the fact that almost all the S_2 state is relaxed to the planar S_1 state. As discussed in the following, the difference in the isomerization quantum yield indicates that another relaxation channel is open in vibrationally excited S_1 states.

With photoexcitation at 280 nm, the molecule gains energy as high as ~35 700 cm^{-1}. Since the energy dissipation to the

surrounding solvent takes place on a time scale of a few tens of picoseconds, almost all energy is still localized in the molecule even after the $S_2 \rightarrow S_1$ relaxation. Since the lifetime of the generated S_1 state is also much shorter than the time scale of the energy dissipation, all the process in the S_1 state is considered to occur while the molecule is vibrationally excited. This argument is experimentally supported by the previous picosecond Raman data, in which high-frequency anti-Stokes S_1 Raman bands were observed with quite high intensity.[20] Therefore, the small isomerization quantum yield obtained with S_2 photoexcitation is attributable to the low isomerization efficiency of the vibrationally excited S_1 state. In other words, the isomerization quantum yield of the "vibrationally excited" S_1 state, which is produced by the $S_2 \rightarrow S_1$ electronic relaxation, is significantly lower than the quantum yield of the "relatively cold" S_1 state that is generated by direct $S_1 \leftarrow S_0$ photoexcitation. In fact, a tendency supporting this idea has been observed in the photochemical experiments of Zimmerman et al.[37] They measured the excitation wavelength dependence of the trans $\rightarrow$ cis isomerization quantum yield and found that the quantum yield decreases with the increase of the excitation energy even within the S_1 absorption band: The isomerization quantum yield obtained with 436-nm excitation is 0.27, but it decreases down to 0.21 at 405-nm excitation. The isomerization quantum yield is determined by the ratio between the isomerization rate and the rate of the other relaxation pathways. Therefore, the isomerization quantum yield that decreases with the increase of the excess energy indicates that the trans $S_1 \rightarrow$ trans S_0 relaxation process is accelerated in the vibrationally excited S_1 state.

The data of the S_1 lifetime also support the acceleration of the $S_1 \rightarrow S_0$ relaxation process in the vibrationally excited S_1 state. The lifetime of the S_1 state that appears after the S_2 excitation (280 nm) was determined to be $\sim$500 fs in the present up-conversion measurement. On the other hand, the lifetime of the S_1 state prepared by the direct red-edge S_1 photoexcitation (503 nm) was reported to be $\sim$2.6 ps.[18] The S_1 lifetime becomes significantly shorter with increase of the excess vibrational energy. Taking account of the decrease of the isomerization quantum yield, it is natural to attribute the shortening of the S_1 lifetime to the acceleration of the $S_1 \rightarrow S_0$ relaxation process in the vibrational excited S_1 state.

Interestingly, the excess energy dependence of the isomerization quantum yield as well as that of the S_1 lifetime vanishes when the rotational motion of azobenzene is blocked by chemical modification. Rau and Lüddecke measured the trans $\rightarrow$ cis isomerization quantum yield of a "blocked" azobenzene and found that the yield is kept almost constant even if the excitation condition is changed: 0.21 for the $S_2(\pi\pi^*) \leftarrow S_0$ excitation and 0.24 for the $S_1(n\pi^*) \leftarrow S_0$ excitation.[4] Lednev et al. performed femtosecond absorption spectroscopy for another blocked azobenzene and reported that the lifetime of the S_1 state appearing after $S_2 \rightarrow S_1$ relaxation is exactly the same as the lifetime of the S_1 azobenzene that is generated by the S_1 red-edge excitation (2.6 ps).[19] These facts suggest that the acceleration of the trans $S_1 \rightarrow$ trans S_0 relaxation in the vibrationally excited S_1 state is due to the opening of a new relaxation channel that is related to the rotational coordinate. It seems that this "rotational" relaxation channel finally produces the trans S_0 state but does not generate the cis isomer.

It should be noted that the vibrationally excited S_1 state we have discussed here may not be mere the "hot" S_1 state in which the vibrational energy is statistically distributed over all the vibrational freedoms. Since the lifetime of the S_1 azobenzene produced by the $S_2 \rightarrow S_1$ electronic relaxation is comparable to a time scale of the intramolecular vibrational redistribution process (IVR), it is likely that the statistical vibrational energy distribution is not achieved in the S_1 state. Therefore, it might be possible that the rotation relaxation channel we argued is open only in the vibrational excited S_1 state before the intramolecular vibration redistribution process.

The time-resolved spectroscopic studies (absorption, fluorescence, and Raman) have successfully revealed photochemical dynamics of azobenzene following S_2 photoexcitation, and they allowed us to consider the isomerization process after S_2 and S_1 photoexcitation in a unified and consistent framework. To rationalize all the spectroscopic and photochemical data, it seems that we need to consider, at least, three relaxation channels in the S_1 state, (1) the inversion isomerization channel, (2) the trans $S_1 \rightarrow$ trans S_0 relaxation channel that is open even in the cold S_1 state, and (3) the trans $S_1 \rightarrow$ trans S_0 rotational relaxation channel that is open only in the vibrationally excited S_1 state. (The radiative decay channel is not important for azobenzene because the fluorescence quantum yield is very low.) The elucidation of these three relaxation channels in the S_1 state is very crucial for full understanding of azobenzene photochemistry, and, we think, it is a central issue for the future experimental and theoretical study of this important molecule.

Acknowledgment. We thank Prof. Igor Lednev for stimulating and fruitful discussion, especially about the relaxation channels in the S_1 state. We also thank Dr. Satoshi Takeuchi for stimulating discussion as well as technical advice. T. F. and S. A. acknowledge the Japan Society for the Promotion of Science for fellowships. This work was partly supported by the Grant-in-Aids for Scientific Research (C) (No. 11640521) from the Japan Society for Promotion of Science.

References and Notes

(1) Liu, Z. F.; Hashimoto, K.; Fujishima, A. *Nature* **1990**, *347*, 658.
(2) Sekkat, Z.; Dumont, M. *Appl. Phys. B* **1992**, *54*, 486.
(3) Ikeda, T.; Tsutsumi, O. *Science* **1995**, *268*, 1873.
(4) Rau, H.; Lüddecke, E. *J. Am. Chem. Soc.* **1982,** *104*, 1616.
(5) Rau, H. *J. Photochem.* **1984**, *26*, 221.
(6) Rau, H.; Yu-Quan, S. *J. Photochem. Photobiol.* **1988**, *A 42*, 321.
(7) Siampiringue, N.; Guyot, G.; Monti, S.; Bortolus, P. *J. Photochem.* **1987**, *37*, 185.
(8) Okamoto, H.; Hamaguchi, H.; Tasumi, M. *Chem. Phys. Lett.* **1986**, *130*, 185.
(9) Biswas, N.; Umapathy, S. *Chem. Phys. Lett.* **1995**, *236*, 24.
(10) Curtis, R. D.; Hilborn, J. W.; Wu, G.; Lumsden, M. D.; Wasylishen, R. E.; Pincock, J. A. *J. Phys. Chem.* **1993**, *97*, 1856.
(11) Armstrong, D. R.; Clarkson, J.; Smith, W. E. *J. Phys. Chem.* **1995**, *99*, 17825.
(12) Monti, S.; Orlandi, G.; Palmieri, P. *Chem. Phys.* **1982**, *71*, 87.
(13) Waldeck, D. H. *Chem. Rev.* **1991**, *91*, 415.
(14) Saltiel, J.; D'Agostino, J.; Magarity, E. D.; Metts, L.; Neuberger, K. R.; Wrighton, M.; Zafirou, O. C. *Org. Photochem.* **1973**, *3*, 1.
(15) Hochstrasser, R. M. *Pure Appl. Chem.* **1980**, *52*, 2683.
(16) Shimojima, A.; Tahara, T. *J. Phys. Chem. B* **2000**, *104*, 9288.
(17) Lednev, I. K.; Ye, T.-Q.; Hester, R. E.; Moore, J. N. *J. Phys. Chem.* **1996**, *100*, 13338.
(18) Lednev, I. K.; Ye, T.-Q.; Matousek, P.; Towrie, M.; Foggi, P.; Neuwahl, F. V. R.; Umapathy, S.; Hester, R. E.; Moore, J. N. *Chem. Phys. Lett.* **1998**, *290*, 68.
(19) Lednev, I. K.; Ye, T.-Q.; Abbott, L. C.; Hester, R. E.; Moor, J. N. *J. Phys. Chem. A* **1998**, *102*, 9161.
(20) Fujino, T.; Tahara, T. *J. Phys. Chem. A* **2000**, *104*, 4203.
(21) Tahara, T.; Hamaguchi, H.; Tasumi, M. *J. Phys. Chem.* **1987**, *91*, 5875.
(22) Tahara, T.; Hamaguchi, H.; Tasumi, M. *Chem. Phys. Lett.* **1988**, *152*, 135.
(23) Tahara, T.; Hamaguchi, H.; Tasumi, M. *J. Phys. Chem.* **1990**, *94*, 170.
(24) Hamm, P.; Ohline, S. M.; Zinth, W. *J. Chem. Phys.* **1997**, *106*, 519.

(25) Takeuchi, S.; Tahara, T. *J. Phys. Chem. A* **1997**, *101*, 3052.
(26) Arzhantsev, S. Y.; Takeuchi, S.; Tahara, T. *Chem. Phys. Lett.* **2000**, *330*, 83.
(27) Engel, P. S.; Steel, C. *Acc. Chem. Res.* **1973**, *6*, 275.
(28) Rau, H. *Angew. Chem., Int. Ed. Engl.* **1973**, *12*, 224.
(29) Struve, W. S. *Chem. Phys. Lett.* **1977**, *46*, 15.
(30) Morgante, C. G.; Struve, W. S. *Chem. Phys. Lett.* **1979**, *68*, 267.
(31) Sarkar, N.; Takeuchi, S.; Tahara, T. *J. Phys. Chem. A* **1999**, *103*, 4808.
(32) Takeuchi, S.; Tahara, T. *Chem. Phys. Lett.* **1997**, *277*, 340.
(33) Takeuchi, S.; Tahara, T. *J. Phys. Chem. A* **1998**, *102*, 7740.
(34) Turro, N. J. *Molecular Photochemistry*; W. A. Benjamin Inc.: Massachusetts, 1965; Chapter 3.
(35) The oscillator strength of the nπ* transition has been reported for gas-phase azobenzene, and it is 0.0071 at 472 K and 0.0077 at 599 K.[39] These values are smaller than the present value that is obtained for the molecule in hexane. This difference probably indicates that the structure of azobenzene in solution is slightly different from that in the gas phase owing to the interaction with solvent molecules.
(36) Birnbaum, P. P.; Style, D. W. G. *Trans. Faraday Soc.* **1954**, *50*, 1192.
(37) Zimmerman, G.; Chow, L. Y.; Paik, U. J. *J. Am. Chem. Soc.* **1958**, *80*, 3528.
(38) Bortolus, P.; Monti, S. *J. Phys. Chem.* **1979**, *83*, 648.
(39) Andersson, J.; Petterson, R.; Tegner, L. *J. Photochem.* **1982**, *20*, 17.